

Optical investigation of the origin of switching conduction in charge-density waves

Naoki Ogawa and Kenjiro Miyano*

Research Center for Advanced Science and Technology, University of Tokyo, Tokyo 153-8904, Japan

(Received 10 February 2004; published 26 August 2004)

Low-temperature dynamical properties of the sliding charge-density wave (CDW) in $K_{0.3}MoO_3$ was investigated using the optical modulation of the phase strain. An intimate relation between switching transition, size effects, and photoeffects was found, and discussed in terms of the plastic ground state of the CDW. Large evolution of the sliding threshold voltage and clear conduction delay were also observed, and manipulated through photoexcitation. Optical excitation is more effective in the plastic state, and it is confirmed that the switching occurs through the inhomogeneous breaking transition of the rigid but fragile CDW.

DOI: 10.1103/PhysRevB.70.075111

PACS number(s): 71.45.Lr, 78.20.-e

I. INTRODUCTION

The charge-density wave (CDW)^{1,2} is condensation of electron-hole pairs with a Peierls gap at the Fermi level. Since electrons directly interact with electric field including light, there have been numerous reports on optical investigation of its physical properties, ranging from classical reflectivity measurements to electromodulated³ and ultrafast pump-probe⁴ spectroscopy, as in other highly correlated materials. However, the number of experiments utilizing light not as “probe” but as “stimulus” has been limited⁵ in comparison with that on superconductors which have the formal analogy with CDW. There are two kinds of low-energy collective excitation in the CDW. The phase mode (phason) is infrared active and the amplitude mode (amplitudon) is normally a Raman mode, but in the presence of impurities it may also become infrared active. Therefore, with optical excitation, these two modes of collective excitation should arise in addition to semiconductorlike single particle excitation above the Peierls gap. In the ultrafast pump-probe measurements, excited quasiparticles induce amplitude oscillations and overdamped phason relaxation of the CDW.⁴ The sliding motion of the CDW can be regarded as phase mode excitation, going along with the amplitude mode at phase slip centers.⁶ Considering the critical behavior in the sliding transition, it is natural to expect a significant change in the dynamics of the CDW by optical excitation.

Switching and hysteresis in I - V curves have been observed in typical sliding CDW materials as $NbSe_3$,⁷ TaS_3 ,⁸ and $K_{0.3}MoO_3$,⁹ and usually become more pronounced at low temperatures. Although the origin of these phenomena has not been clearly understood yet, various forms of CDW plasticity and inhomogeneity, including a nucleation of phase dislocation¹⁰ and shear deformation between CDW chains or two-dimensionally coupled sheets,¹¹ have been proposed to account for the properties of the creep motion and the transition between creep to slide at the threshold voltage V_s . In the sliding CDW system, the dynamics of the CDW at high temperatures are relatively well explained by the extended Fukuyama-Lee-Rice (FLR) model¹² including screening by uncondensed carriers. However, this model neglects the CDW amplitude fluctuation, such as phase slippages, and qualitative deviations have been reported experimentally at lower temperatures, where the CDW is well described as a

plastic medium.¹⁰ At these temperatures, the number of free carriers become too small to screen elastic phase deformations (called Coulomb hardening).^{1,13} A number of evidences have been reported about the transition from screened to unscreened response.¹⁴ Recently, the existence of two relaxation processes and their close relationship with the sliding threshold field were reexamined by Starešinić *et al.*¹⁵ through low frequency dielectric spectroscopy and thermally stimulated depolarization experiments. They observed splitting of the relaxational spectrum into two branches on decreasing temperature and the subsequent freezing of one process at around 23 K. The high-temperature process was ascribed to the dynamics of the collective elastic deformations of the CDW phase, whose relaxation time increased continuously with decreasing temperature, whereas the low temperature process was assigned to the remaining degrees of freedom after the elastic ones are frozen out, i.e., topological or plastic deformations of the CDW phase, such as solitons,¹⁶ domain walls, and dislocation loops.¹⁷ Their results indicate that the high-temperature polarization occurs overcoming the elastic pinning, while the low-temperature response appears through the breaking of the CDW or nucleation of the phase defects. These two relaxation processes coexist around 25–40 K. In the plastic state, it is important that the relaxed particles do not stay near the Peierls gap edge as semiconductorlike electrons and holes. Instead they acquire a form of the amplitude soliton with smaller energy.¹⁸ With the amplitude of the CDW passing through zero, the amplitude soliton becomes a static phase slip center thus playing a key microscopic role in effects of depinning.

We have reported that the photoexcitation drastically changes the sliding dynamics of $K_{0.3}MoO_3$ at low temperatures.¹⁹ With photoillumination, both the creep current and the sliding threshold V_s increase. In the sliding phase slightly above V_s , the motion of the CDW can be totally arrested by illumination. The photoeffects can be clearly distinguished from heating effects of illumination and are persistent. These effects can be observed with photon energy exceeding the Peierls gap and in the temperature range below ~ 25 K. We have interpreted that the optical modulation of CDW phase strain mainly causes these effects in the following way. With external electric field, the CDW phase deforms around a pinning site. If photons happen to hit the condensate near the pinning site, quasiparticles are excited above

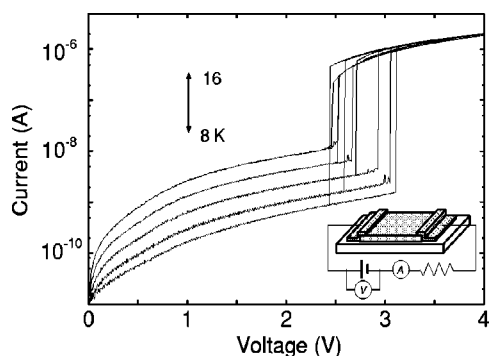


FIG. 1. Temperature dependence of the I - V curves. The temperature increment was 2 K. The inset shows the electrical contact arrangement in which the protection resistor is present.

the Peierls gap. Then the excited quasiparticles releases their energy through electron-electron and electron-phonon interaction, and finally recondense into the CDW with less deformed phase configuration, which should be energetically more favorable. This process results in effective phase slips and stress relaxation, which stabilize the creep phase, and the sliding transition is postponed to a higher voltage. The photoinduced change of the CDW phase deformation was confirmed by high-resolution x-ray diffraction study.²⁰

Many unique properties of the CDW arise from the nearly degenerate large number of metastable states in the phase deformation and its glassy relaxation. However, it has been believed that the only way to remove the phase strain is by thermal cycling. This restriction can now be overcome by the photoexcitation process. In this article, we investigate the relation between the switching transition, size effects, and the Coulomb hardening in the sliding conduction through optical excitation experiments.

II. EXPERIMENTS AND DISCUSSION

A. Sample preparation

Single crystals of $\text{K}_{0.3}\text{MoO}_3$ were synthesized by means of the electrolytic reduction of $\text{KMoO}_4\text{-MoO}_3$ melt.²¹ A typical sample size is $1.3 \times 1 \times 0.2 \text{ mm}^2$ after the cleavage. The samples were glued to sapphire plates and indium electrodes with several gap separation were evaporated onto the surface. The measurements have been performed in a two-probe geometry. The resistance of the contacts was much smaller than the sample resistance.

B. I - V characteristics

Temperature variation of the I - V curves of a sample with an electrode gap of $600 \mu\text{m}$ is shown in Fig. 1. A protection resistor of $1 \text{ M}\Omega$ was inserted to the circuit. Without this resistor, the current exceeded milliamperes at V_s , and the experimental results became more and more irreproducible due to the Joule heating. As is often observed in $\text{K}_{0.3}\text{MoO}_3$, switching and hysteresis behavior at V_s is obvious. The I - V response at low bias voltage is already nonlinear, and dominated by the creep motion rather than the thermally excited normal carriers across the Peierls gap.²² The current hysteresis

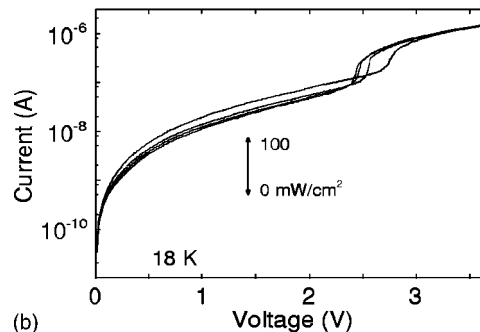
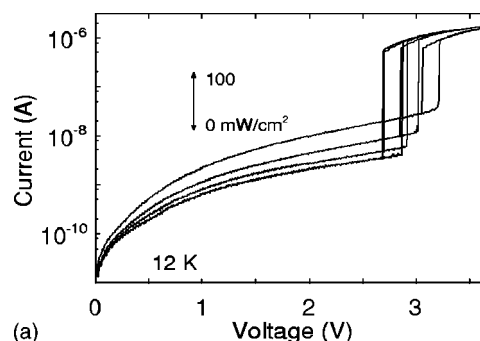


FIG. 2. Illumination intensity dependence of the I - V curves measured at (a) 12 and (b) 18 K. Light intensity was increased as 0, 6.125, 25, 100 mW/cm^2 . In (b), the hysteresis is small and not depicted for clarity.

at low bias was negligible, assuring that the measurement was performed in nearly thermal equilibrium state. With increasing temperature, the creep current increased and the V_s decreased. The hysteresis loop became smaller and the transition at V_s began to be rounded. The switching motion and large hysteresis were observed below $\sim 25 \text{ K}$.

I - V responses under light illumination (photon energy $= 2.33 \text{ eV}$) measured at 12 and 18 K are shown in Fig. 2. The incident polarization is parallel to the chain structure (b direction) hereafter, although no dependence on polarization was observed, which is consistent with the amplitude mode excitation observed in pump-probe experiments.⁴ At 12 K, the creep current increased with illumination, whereas V_s also increased showing clear contrast with its temperature dependence (Fig. 1). At 18 K, the effects of optical excitation became smaller both in the creep current and in the shift of V_s . These photoeffects can be seen only below $\sim 25 \text{ K}$, where the switching and hysteresis in the I - V curves can be observed. This is the same temperature range in which the elastic degrees of freedom of the CDW should be frozen out. If we assume that the temperature variation of the I - V curves is due mainly to the difference in the number of normal carriers, the change of only 3% [$n(18 \text{ K})/n(12 \text{ K})$, assuming activation behavior] in thermally excited carriers results in the drastic change in the switching motion as shown in Fig. 2. Therefore it is natural that the small number of photoexcited carriers induce a large variation in the switching transition. However, the photoeffect is different from the temperature effect in that the temperature should shift the ground state of the CDW from plastic to elastic, whereas the photoexcitation keeps the ground state plastic, because the lifetime

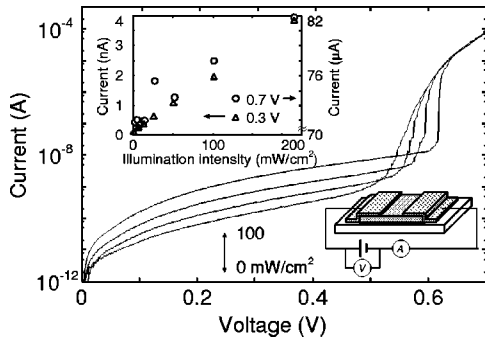


FIG. 3. I - V curves of a sample with a small electrode gap under light illumination at 6.2 K. The hysteresis at V_s is relatively small and not shown. Light intensity was increased as 0, 6.125, 25, 100 mW/cm^2 . Upper inset shows the illumination intensity dependence of creep (triangle, at 0.3 V) and slide current (circle, at 0.7 V). Lower inset shows the contact arrangement.

of the quasiparticles should be very short,⁴ and affects only a small part of the sample [near the surface within the penetration depth of the light (~ 100 nm)²³].

Figure 3 shows the evolution of the I - V curves of a sample with a smaller electrode gap of $50 \mu\text{m}$ under laser illumination of varying intensity. The data were measured at 6.2 K. In this case, no protection resistor was inserted to the circuit. In contrast to the sample with a wider gap, a clear switching behavior is absent in the I - V curve in the dark, which is consistent with several reports on size effects. Possible cause for the difference will be discussed later. As we have fabricated many samples with various electrode gaps, most of the samples with the gap smaller than $200 \mu\text{m}$ showed the rounded I - V curves. On illumination with laser light, however, the switching behavior is recovered. As is the case with the sample with a wider gap, the increase of the creep current and pronounced shift of V_s as a function of the light intensity were observed. Both in the creep and the slide regime, current increased linearly with illumination intensity as shown in the upper inset of Fig. 3.

Finite size effects have been playing a key role in understanding the CDW physics, since the phase coherence length extends to the order of micrometers and the collective dynamics of the CDW sensitively depends on it. The photoinduced recovery of the switching in the I - V curve (Fig. 3) shows the intimate coupling between the size effects, the switching transition, and the photoeffects. Previous studies on finite size effects show a crossover from three-dimensional to two-dimensional²⁴ or from two-dimensional to one-dimensional²⁵ collective pinning by reducing the thickness and the width of the crystal. In these experiments, rounding of the I - V curve at the threshold was observed and explained by the thermal fluctuation due to the reduction of total energy in the phase coherent domain. With decreasing the electrode gap ($\leq 100 \mu\text{m}$ for TaS_3), the blurring of the dV/dI - I curve was also reported²⁶ and ascribed to the inhomogeneity of the electric field and the contact-related strain accumulation.

In $\text{K}_{0.3}\text{MoO}_3$, the contact-related strain (or phase slip region²⁷) extends over $100 \mu\text{m}$ (Ref. 28) at 80 K. Although the appearance of a new ground state of the CDW has been

proposed at low temperatures as discussed above, the rounded I - V curves in the $50 \mu\text{m}$ -gap sample (Fig. 3) clearly show the existence of the contact-related strain in the same scale. This strain increases the phase slip rate²⁹ and the inhomogeneity in the conduction, leading to a partial sliding motion of the CDW.¹¹ This partial sliding should be accompanied by continuous nucleation of phase dislocations between mobile and immobile regions or at contacts. This is consistent with the highly dissipative sliding motion in the small-gap sample, in which the current growth is moderate and the I - V curve can be measured without a protection resistor. In contrast, the large-gap sample must be protected by a series resistor against the sudden increase of the current in the sliding regime, and its low sliding resistance is probably due to the large coherence, barely disturbed by the phase defects, and the large sliding volume in the depth direction of the sample. If this is the case, the photoinduced recovery of the switching behavior in the small-gap sample signifies the reduction of the phase defects and the increase of the phase coherence. This is consistent with the linear increase of both the creeping and sliding current by illumination (Fig. 3 upper inset). The nonlinear increase of V_s with illumination intensity¹⁹ may have its origin in the competition between the creation of the phase defects and their annihilation by optical excitation. However, we cannot estimate the efficiency of the optical excitation because the quantum efficiency and also the conduction cross section are not clear at this moment.

Unlike many other CDW materials with a needlelike crystal shape, $\text{K}_{0.3}\text{MoO}_3$ grows three dimensionally to a large volume. The problem of inhomogeneity is thus more severe and has been preventing the measurements of the interference phenomena such as the narrow band noise (NBN) and the mode locking. The observation of NBN in thinned samples of $\text{K}_{0.3}\text{MoO}_3$ (Ref. 30) indicates that the CDW in the cleavage plane [$b-(a+2c)$] is relatively coherent, and the coupling in the depth direction disturbs the coherent sliding motion. Considering the weakest electronic coupling in the depth direction³¹ and our contact geometry, the sliding motion should be triggered by the depinning of the two-dimensionally coupled CDW sheet near the sample surface,¹¹ dragging the neighboring sheets and chains. This model can partly explain the sensitive dependence of the bulk sliding conduction on light illumination. As the elastic degrees of freedom is taken over by the plastic one at these temperatures, the notion of FLR length cannot be applied directly to the observed size effects.

C. Start-stop measurement

CDW is a model system of the boundary friction inside a crystal. The pinning in the rest state and the damping in the sliding state correspond to the static friction and the kinetic friction, respectively. In usual boundary friction systems, the coefficient of static friction increases logarithmically with a duration of contact, which has been explained by the increase of the “real” contact area.³² However, exponential time dependences of the static friction force are known in cold works of metals³³ and lubricated boundary frictions,³⁴ in

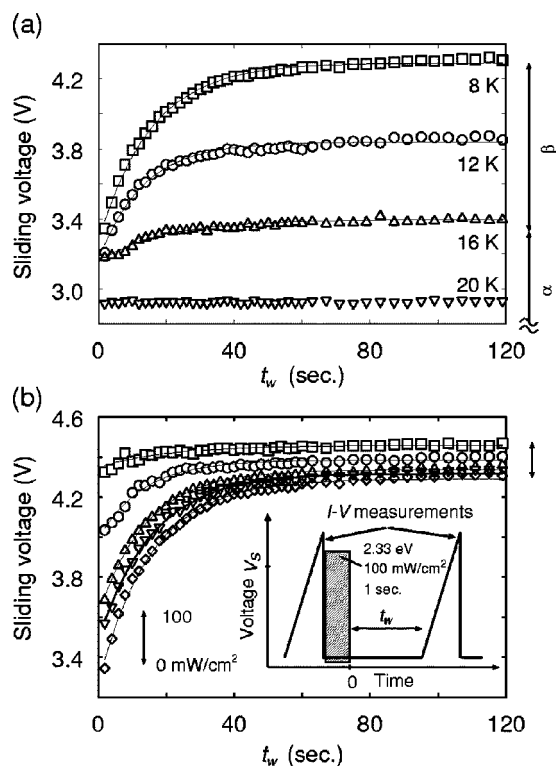


FIG. 4. (a) Time evolution of the threshold voltage V_s after a sliding motion measured at low temperatures. Vertical arrows show the definition of α and β in Eq. (1) for the case of 8 K. (b) Illumination intensity dependence of the time evolution of V_s measured at 8 K. Light intensity was increased as 0, 12, 25, 50, 100 mW/cm². Vertical arrow on the right indicates the change which can be induced only through optical excitation. Solid lines in the plots are fit with Eq. (1). Inset shows the experimental procedure. See text for detail.

which respective time evolution is explained by the recovery of dislocations or interdiffusion of the chains of grafted molecules. In other words, the time evolution of the static friction force depends on the microscopic mechanisms of the phenomena occurring at boundaries. In CDW systems, several experiments on the time evolution of V_s after the termination of sliding motion have been reported³⁵ and explained in terms of the relaxation of the phase deformation or the thermal diffusion of impurities.³⁶

In studying the waiting-time dependence of V_s after a momentary slide,³⁷ we found a large evolution of V_s below 20 K. The data were measured with large-electrode-gap samples hereafter. The experimental procedure was as follows [Fig. 4(b) inset]: Without laser irradiation, we initiated a sliding of the CDW by applying a large electric field to prepare the sample in a highly distorted state (which is the same as the I - V measurement over V_s). Shortly after, we switched-off the electric field, and then measured the V_s after some waiting time t_w .

In the dark at 8 K, V_s increased about 20% within 60 s [Fig. 4(a)], and the waiting time dependence can be well fitted with an exponential function

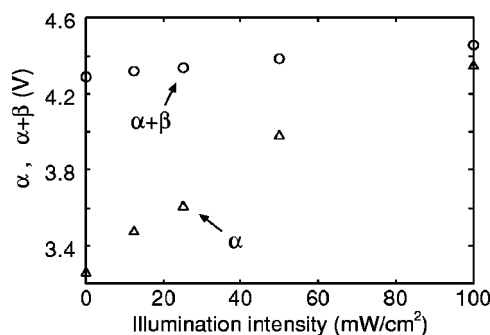


FIG. 5. Illumination intensity dependence of α and $\alpha + \beta$ in Eq. (1).

$$f(t_w) = \alpha + \beta[1 - \exp(-t_w/\tau_w)]. \quad (1)$$

The time constant τ_w is about 15 s, which is much smaller than the observed phase relaxation time in the x-ray experiments³⁸ at these temperatures. The temperature dependence of this time constant was not clear because of the limited temperature range.

We applied laser light (2.33 eV, 100 mW/cm²) just after the strain induction. Immediately after illuminating the sample for 1 s, V_s tends to get higher in accordance with the illumination intensity [Fig. 4(b)]. It then saturates exponentially within a fixed time constant τ_w , although the saturation values depend on the light intensity. Figure 5 shows the illumination intensity dependence of the initial threshold voltage α and the final voltage ($\alpha + \beta$). Both increased almost linearly with illumination intensity.

We assume that the observed time dependence can be accounted for by two factors. (1) The stress-dependent pinning potential is affected by the partial removal of the stress through thermal relaxation or photoexcitation and (2) the static friction between mobile and immobile regions in the sample increases, for example, as the phase dislocations are annihilated. Both come into play in the relaxation of the phase strain. Because the photoeffect is fast,¹⁹ we do not take the mobile impurity scenario into consideration. The relaxation of the phase deformation has been modeled as relaxation in a hierarchy of potential barriers as shown in Fig. 6.³⁹ The sliding motion induces large phase deformation, and its decay occurs sequentially as follows: (1) initial relaxation to the nearest metastable state ($\sim \exp[-(t/\tau)^\beta]$), (2) escape over low energy barriers [$(\ln t)^{-\alpha}$], (3) relaxation down a hierarchy of barriers. Logarithmic or stretched exponential time dependence of the depolarization has been reported experimentally.⁴⁰ In this model, photoexcitation promotes the relaxation, further than the thermal relaxation, down the hierarchy of potential barriers to the ground state, through effectively reducing the height of potential barriers between metastable wells. Here, thermal relaxation corresponds to the time-dependent increase of V_s in Fig. 4(a), and the additional relaxation can be observed in the change of ($\alpha + \beta$) as indicated with a vertical arrow in Fig. 4(b). This is a clear example of the optical control of the CDW internal deformation.

As introduced formerly, two modes of relaxation have been distinguished in the frequency-dependent dielectric

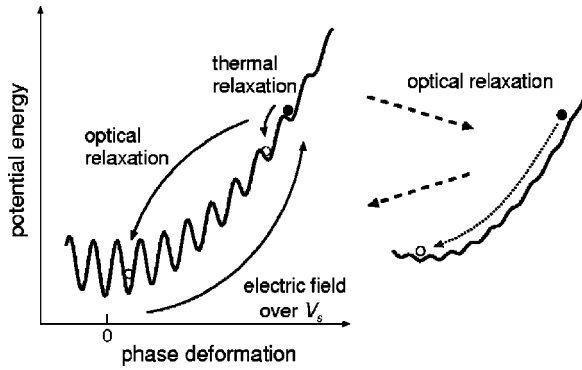


FIG. 6. Illustration of a potential landscape and internal degrees of freedom (deformation). A circle represents a state of the system. With electric field larger than V_s , the phase deforms and simultaneously the potential energy increases through the elastic distortion or the creation of the phase defects. The system is then trapped in a nearby potential well and begins to relax thermally down the hierarchy. Optical excitation effectively reduces the barrier height and promotes the relaxation, which should be deeper in the potential hierarchy and faster than that of the thermal relaxation process.

measurements.¹⁵ The high-temperature mode freezes out around 23 K, leading to an infinite relaxation time for this mode. On the other hand, the relaxation time of the low-temperature mode is estimated to be 10 s around 15 K,¹⁵ which nicely coincides with the observed time constant τ_w . In addition, large time evolution of V_s has been observed only below 20 K, the same temperature range where switching and hysteresis at V_s can be seen. This confirms that the sliding transition, accompanied by a switching and the time evolution of V_s , have their main origin in the low-temperature mode of relaxation, i.e., in the plastic deformation of the CDW. Optical instant modulation of the CDW phase strain can also be clearly observed in the delayed conduction as shown below.

D. Conduction delay

With controlled illumination, we can prepare a phase distribution with a varying degree of relaxation, which is desirable in the deformation-sensitive experiments. One of the unique phenomena observed in the sliding CDW system is the delayed conduction. If a voltage (or current) step slightly larger than V_s is applied, the sliding motion starts with a certain delay in time. Such delayed conduction can be observed in many driven dynamical systems as Josephson tunnel junctions⁴¹ and phase-slip centers in high- T_c superconductors.⁴² In CDW systems, the delay time τ_d has statistical distributions with sensitive dependence on the initial phase configuration, and is considered as the time during which the internal phase strain evolves sufficiently large to tear the CDW.⁴³ Several experiments^{44–46} and numerical studies^{47,48} have been reported, but the microscopic mechanism has not been elucidated.

Examples of the conduction delay measured at 12 K are shown in Fig. 7. The threshold voltage V_s of this sample was about 2.6 V at this temperature, and current was monitored with a reference resistor of 1 M Ω inserted in the circuit. We

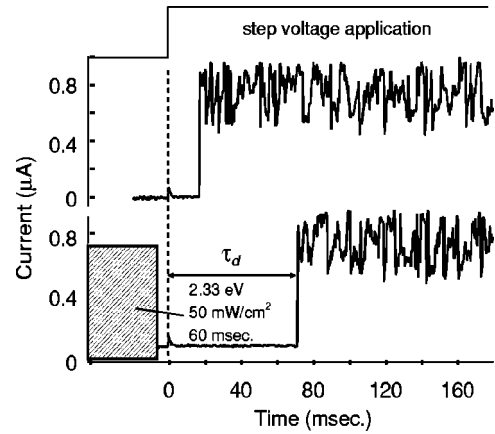


FIG. 7. Procedure and examples of the conduction delay with and without light illumination measured at 12 K. When we illuminate the sample before the step voltage application, the delay time increases depending on the illumination intensity and the bias voltage. Small polarization current at time 0 and large current noise in the sliding regime can be seen.

created a phase distortion in the sample with a voltage pulse larger than V_s , and subsequently applied a rectangular pulse of fixed voltage to measure the conduction delay. The delay time τ_d was measured 2048 times at each condition. We have observed clear delay with the samples showing switching conduction.

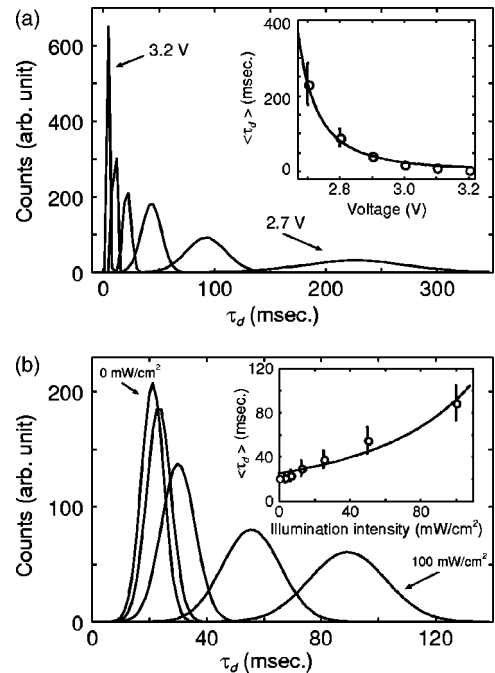


FIG. 8. (a) Distribution of the delay time τ_d with respect to the applied voltage. Voltage increment was 0.1 V. Inset shows the mean value $\langle \tau_d \rangle$ vs voltage. The solid line indicates its power law dependence. (b) Illumination intensity dependence of the distribution of τ_d . The light intensity was increased as 0, 12.5, 25, 50, 100 mW/cm². Inset shows the mean value $\langle \tau_d \rangle$ vs illumination intensity. Solid line is from Eq. (3). Vertical bars in the insets indicate the FWHM of the distribution.

The bias dependence of τ_d is shown in Fig. 8(a). At around V_s , τ_d has a broad distribution with slight asymmetry in its profile, which reflects both the distribution of the initial phase configuration⁴⁹ and the relaxation time.⁵⁰ With increasing bias voltage, τ_d and its distribution become smaller. The mean value $\langle \tau_d \rangle$ as a function of applied bias is shown in the inset of Fig. 8(a), which obeys the power law

$$\tau_d \propto \left(\frac{V}{V_s} - 1 \right)^{-\delta}, \quad (2)$$

with $\delta=2.03$. This is consistent with previous reports on NbSe₃ (Ref. 46) (some samples obey $\delta \sim 2$) and on K_{0.3}MoO₃,⁴⁵ but shows some deviations from the theoretical predictions from the amplitude-collapse model ($\delta \sim 0.5$) and the mean-field phase slip model ($\delta \sim 1$).⁴⁸

When we illuminate the sample (2.33 eV, 60 ms) just before the application of a voltage pulse (Fig. 7), both τ_d and its fluctuation increase monotonically with light intensity [Fig. 8(b)], clearly showing the persistence of the photoeffect as has been utilized in optical memory effects.⁵¹ This result can be explained by the photoinduced increase of V_s as discussed in the previous section, which reduces the effective driving force ($V/V_s - 1$). If we assume a linear dependence of V_s on illumination intensity as can be seen in Fig. 5, the increase of τ_d can be well expressed with a function

$$\tau_d \propto \left(\frac{V}{V_s(I)} - 1 \right)^{-2}, \quad (3)$$

as shown in the inset of Fig. 8(b). Then, the problem again comes to the mechanism of the photoinduced increase of V_s and also to the origin of the broad distribution of τ_d . The large delay-time distribution can be found in several physical systems,⁵² and usually explained by the thermally activated escape from the metastable potential wells.⁵³ Although this distribution has been ascribed to the initial phase configura-

tion in the CDW,⁴⁶ there are many other possible explanations such as the Wigner time delay in a quantum mechanical scattering⁵⁴ and the depinning process in boundary friction systems.⁵⁵ The photoinduced increase of the conduction delay shows its clear relation with phase deformation. However the microscopic measurements on the mechanism of depinning is indispensable to totally understand the dynamics of CDW.

III. CONCLUSION

We have found a coupling between the switching transition, conduction delay, size effects, and photoexcitation effects in the CDW conductor K_{0.3}MoO₃. The contact-related strain disturbs the coherent motion of the CDW and should lead to inhomogeneous conduction, fragmentation, and dissipation in the sliding CDW. The photoexcitation removes the phase strain and recovers the coherence of the CDW. We also observed the time evolution of V_s after the termination of sliding motion, which can be promoted through optical excitation. We conclude that various unusual properties in the CDW dynamics at low temperature are the basic features of the plastic ground state after the freezing out of elastic degrees of freedom. We believe that we can prepare nearly as-cooled state of the CDW phase configuration by optical excitation, which is indispensable for the controlled experiments. Photoexcitation is thus an effective tool to investigate the low-temperature dynamics of the CDW.

ACKNOWLEDGMENTS

We thank Professor S. Brazovskii and Professor H. Matsukawa for valuable comments and discussions, and Dr. R. Kondo for his help in sample preparation. This work was supported by JSPS Research Fellowships for Young Scientists and by JSPS KAKENHI (Grant No. 15104006).

*Electronic address: stream@myn.rcast.u-tokyo.ac.jp

¹ For a review, see for example, G. Grüner, Rev. Mod. Phys. **60**, 1129 (1988); *Density Waves in Solids* (Addison-Wesley, Longmans, MA, 1994).

² *Charge Density Waves in Solids*, edited by L. Gor'kov and G. Grüner (Elsevier, Amsterdam, 1989).

³ M. E. Itkis, B. M. Emerling, and J. W. Brill, Phys. Rev. B **56**, 6506 (1997).

⁴ J. Demsar, K. Biljakovic, and D. Mihailovic, Phys. Rev. Lett. **83**, 800 (1999); J. Demsar, D. Mihailovic, V. V. Kabanov, and K. Biljakovic, cond-mat/0401059 (unpublished), and references therein.

⁵ For example, M. E. Itkis, F. Ya. Nad', and V. Ya. Pokrovskii, Sov. Phys. JETP **63**, 117 (1986).

⁶ B. Gorshunov, S. Haffner, M. Dressel, B. Lommel, F. Ritter, and W. Assmus, J. Phys. IV **12**, PR9-81 (2002).

⁷ R. P. Hall, M. F. Hundley, and A. Zettl, Phys. Rev. Lett. **56**, 2399 (1986).

⁸ M. E. Itkis, F. Ya. Nad', and P. Monceau, J. Phys.: Condens.

Matter **2**, 8327 (1990).

⁹ Atsutaka Maeda, Masaya Notomi, and Kunimitsu Uchinokura, Phys. Rev. B **42**, 3290 (1990).

¹⁰ For a review, S. Brazovskii and T. Nattermann, cond-mat/0312375 (unpublished).

¹¹ Valerii M. Vinokur and Thomas Nattermann, Phys. Rev. Lett. **79**, 3471 (1997).

¹² H. Matsukawa, J. Phys. Soc. Jpn. **57**, 3463 (1998).

¹³ A. Virosztek and K. Maki, Phys. Rev. B **48**, 1368 (1993).

¹⁴ B. Hennion, J. P. Pouget, and M. Sato, Phys. Rev. Lett. **68**, 2374 (1992).

¹⁵ D. Staresinic, K. Bijakovic, W. Brutting, K. Hosseini, and P. Monceau, J. Phys. IV **12**, Pr9-15 (2002); for earlier studies, F. Ya. Nad' and P. Monceau, Solid State Commun. **87**, 13 (1993); F. Ya. Nad' and P. Monceau, J. Phys. IV **3**, 343 (1993).

¹⁶ M. J. Rice, A. R. Bishop, J. A. Krumhansl, and S. E. Trullinger, Phys. Rev. Lett. **36**, 432 (1976).

¹⁷ P. A. Lee and T. M. Rice, Phys. Rev. B **19**, 3970 (1979).

¹⁸ S. Brazovskii, in Ref. 2, p. 425.

- ¹⁹N. Ogawa, A. Shiraga, R. Kondo, S. Kagoshima, and K. Miyano, Phys. Rev. Lett. **87**, 256401 (2001).
- ²⁰N. Ogawa, Y. Murakami, and K. Miyano, Phys. Rev. B **65**, 155107 (2002).
- ²¹A. Wold, W. Kunnmann, R. J. Arnott, and A. Ferretti, Inorg. Chem. **3**, 545 (1964).
- ²²S. G. Lemay, R. E. Thorne, Y. Li, and J. D. Brock, Phys. Rev. Lett. **83**, 2793 (1999).
- ²³L. Degiorgi, B. Alavi, G. Mihaly, and G. Grüner, Phys. Rev. B **44**, 7808 (1991).
- ²⁴J. McCarten, D. A. DiCarlo, M. P. Maher, T. L. Adelman, and R. E. Thorne, Phys. Rev. B **46**, 4456 (1992).
- ²⁵E. Slot, H. S. J. van der Zant, K. O'Neill, and R. E. Thorne, Phys. Rev. B **69**, 073105 (2004).
- ²⁶D. V. Borodin, S. V. Zaïtsev-Zotov, and F. Ya. Nad', Sov. Phys. JETP **63**, 184 (1986).
- ²⁷S. G. Lemay, M. C. de Lind van Wijngaarden, T. L. Adelman, and R. E. Thorne, Phys. Rev. B **57**, 12 781 (1998).
- ²⁸B. M. Emerling, M. E. Itkis, and J. W. Brill, Eur. Phys. J. B **16**, 295 (2000).
- ²⁹S. G. Lemay, K. O'Neill, C. Cicak, and R. E. Thorne, Phys. Rev. B **63**, 081102 (2001).
- ³⁰M. F. Hundley and A. Zettl, Phys. Rev. B **39**, 3026 (1989).
- ³¹The anisotropy in conductivity (σ_b/σ_{2a-c}) is about 1000/1 at room temperature and can be much larger at low temperatures.
- ³²Bo N. J. Persson, *Sliding Friction: Physical Principles and Applications* (Springer Verlag, Berlin, 1998).
- ³³M. O. Kornfeld, Phys. Z. Sowjetunion **6**, 239 (1934).
- ³⁴B. N. J. Persson, Phys. Rev. B **55**, 8004 (1997).
- ³⁵*Low-Dimensional Electronic Properties of Molybdenum Bronzes and Oxides*, edited by C. Schlenker (Kluwer, Dordrecht, 1989), p. 197.
- ³⁶J. C. Gill, Phys. Rev. B **53**, 15 586 (1996).
- ³⁷C. Caroli, T. Baumberger, and L. Bureau, J. Phys. IV **12**, Pr9-269 (2002).
- ³⁸L. Mihaly, K.-B. Lee, and P. W. Stephens, Phys. Rev. B **36**, 1793 (1987).
- ³⁹P. B. Littlewood, Phys. Rev. B **33**, 6694 (1986); P. B. Littlewood and R. Rammal, *ibid.* **38**, 2675 (1988).
- ⁴⁰For example, Z. Z. Wang and N. P. Ong, Phys. Rev. B **35**, 5896 (1987).
- ⁴¹T. A. Fulton and L. N. Dunkleberger, Phys. Rev. B **9**, 4760 (1974).
- ⁴²F. S. Jelila, J.-P. Maneval, F.-R. Ladan, F. Chibane, A. Marie-de-Ficquelmont, L. Méchin, J.-C. Villégier, M. Aprili, and J. Lesueur, Phys. Rev. Lett. **81**, 1933 (1988).
- ⁴³J. Levy and M. S. Sherwin, Phys. Rev. B **43**, 8391 (1991).
- ⁴⁴A. Zettl and G. Grüner, Phys. Rev. B **26**, 2298 (1982).
- ⁴⁵A. Maeda, Tatsuo Furuyama, and Shoji Tanaka, Solid State Commun. **55**, 951 (1985).
- ⁴⁶Jeremy Levy and Mark S. Sherwin, Phys. Rev. B **48**, 12 223 (1993).
- ⁴⁷L. Mihaly, Ting Chen, and G. Grüner, Solid State Commun. **61**, 751 (1987).
- ⁴⁸Steven H. Strogatz and Robert M. Westervelt, Phys. Rev. B **40**, 10 501 (1989).
- ⁴⁹Pere Colet and Kurt Wiesenfeld, Phys. Rev. A **46**, 4676 (1992).
- ⁵⁰B. Castaing and J. Souletie, J. Phys. I **1**, 403 (1991).
- ⁵¹N. Ogawa and K. Miyano, Appl. Phys. Lett. **80**, 3225 (2002).
- ⁵²For example, Richard F. Voss and Richard A. Webb, Phys. Rev. Lett. **47**, 265 (1981).
- ⁵³Hermann Grabert, Peter Olschowski, and Ulrich Weiss, Phys. Rev. B **36**, 1931 (1987), and references therein.
- ⁵⁴C. J. Bolton-Heaton, C. J. Lambert, Vladimir I. Fal'ko, V. Prigodin, and A. J. Epstein, Phys. Rev. B **60**, 10 569 (1999).
- ⁵⁵B. N. J. Persson, Phys. Rev. B **51**, 13 568 (1995).